Revision 1

Correlation between Hinckley index and stacking order–disorder in kaolinite

WENXIU RAO[1, #], XIN LIU[1, #], GUOCHENG LV[1, *], MENG LIU[1], LIJUAN WANG[1], JINAN NIU[2], ZHAOHUI LI[3], LIBING LIAO[1]

[1] Engineering Research Center of Ministry of Education for Geological Carbon Storage and Low Carbon Utilization of Resources, Beijing Key Laboratory of Materials Utilization of Nonmetallic Minerals and Solid Wastes, National Laboratory of Mineral Materials, School of Materials Science and Technology, China University of Geosciences (Beijing), 100083, China

[2] School of Materials and Physics, China University of Mining and Technology, Xuzhou 221116, China

[3] Geosciences Department, University of Wisconsin-Parkside, Kenosha, WI 53144, USA

[#] These authors contributed equally to this work and should be considered co-first.

ABSTRACT

Hinckley index (Hi) can be used to characterize the crystallinity of kaolinite. Stacking order–disorder in kaolinite can considerably affect its crystallinity. However, the correlation between Hi and stacking order–disorder in kaolinite has not been reported thus far. Herein, the correlation between stacking order–disorder in kaolinite and Hi was investigated via experiments, molecular simulation, and structure refinement. First, we experimentally discovered that the stacking order–disorder in kaolinite changed the relative position between two adjacent structural layers, majorly affecting interlayer forces. When the kaolinite layers are orderly stacked, the interlayer force is higher and the stacking lattice energy is lower. The lattice energy of kaolinite in different stacking states

was simulated and analyzed using first-principles calculation. It was determined that the kaolinite layers are orderly stacked when two kaolinite layers have zero shift and disorderly stacked otherwise. Finally, through structural refinements, we proposed a new crystallinity index based on stacking order–disorder in kaolinite (crystallinity index based on stacking, CIS). CIS was well fitted to Hi (R^2 = 0.986), proving that kaolinite crystallinity, characterized by Hi, is essentially the ratio of orderly stacking to total stacking (the sum of ordered and disordered stacks). Furthermore, measuring Hi is difficult when kaolinite crystallinity is poor; however, CIS can be used alternatively. This study of the crystallinity of kaolinite will have important significance for its industrial application.

Keywords: kaolinite, stacking, order–disorder, structure refinement, crystallinity index, first-principles calculation

INTRODUCTION

Kaolinite is widely used in ceramics (Hammas et al. 2020), paper-making (Guo et al. 2020), rubber (Qin et al. 2021), petrochemicals (Liu et al. 2020), coatings (Zhang et al. 2021b), and refractory materials (Indahwati et al. 2020) owing to its excellent physical and chemical properties (Ahmad 2020; Gu et al. 2020; Whittaker 1939; Więckowski and Wiewióra 1976). The crystallinity of kaolinite can reflect its physical and chemical properties, such as whiteness (mainly Fe content; Ahmadson et al. 1954), hardness (Fernandez et al. 2011), viscosity (Zhou and Ling 1991), particle size (Zadvernyuk et al. 2021), and chemical stability (Liu et al. 2021). Therefore, the crystallinity of kaolinite is often used to characterize its performance in industrial applications. However, although the world's kaolinite reserves are rich, the crystallinity of kaolinite from diverse origins varies

This is the peer-reviewed, final accepted version for American Mineralogist, published by the Mineralogical Society of America.
The published version is subject to change. Cite as Authors (Year) Title. American Mineralogist, in press.
DOI: https://doi.org/10.2138/am-2022-8830. http://www.minsocam.org/

considerably (Cheng et al. 2018). Therefore, the selection of kaolinite considerably impacts the performance of products. Although kaolinite can be modified by heat, acid, and ball milling to adjust its crystallinity (Murray and Lyons 1960), there is no theoretical guidance for this conclusion. Therefore, to efficiently utilize kaolinite resources, it is necessary to study their crystallinity.

The crystallinity of kaolinite is mainly related to the stacking order–disorder. Kaolinite ($Al_4[Si_4O_{10}](OH)_8$) (Pauling 1930) is a typical 1:1 dioctahedral layered silicate mineral stacked in layers along the *c*-axis and comprising SiO_4 tetrahedral sheets and AlO_6 octahedral sheets (a = 5.1577 Å, b = 8.9417 Å, c = 7.3967 Å, $\alpha = 91.672^{o}$, $\beta = 104.860^{o}$, and $\gamma = 89.898^{o}$) (El-Sayed et al. 1990). Kaolinite is very fine grained, so powder X-ray diffraction (XRD) is the most practical and convenient method for characterizing its crystal structure (Kogure 2011). Many kaolinite crystallinity indexes determined by XRD have been reported, including Hi (Hinckley 1963), Range and Weiss (Range and Weiss 1969), Liétard (Liétard 1977), Stoch (Stoch 1974), Hughes and Brown (Hughes and Brown 2010), Amigó (Amigó et al. 1994), Aparicio-Galán-Ferrell (Aparicio et al. 2006), and "expert system" (Plançon and Zacharie 1990). Hi is the most widely used index (Bergaya and Lagaly 2013), and it is calculated based on the intensity ratio of (110) and ($11\bar{1}$) XRD peaks of kaolinite (Figure 1). The higher the Hi value, the more ordered the kaolinite and the higher its crystallinity. Kaolinite with different crystallinities have different characteristics of XRD peaks, which are mainly reflected in the intensity changes of (110) and ($11\bar{1}$) peaks in the range of 19°–33° (2θ) and the morphological changes of diffraction peaks in the range of 34°–40°. The higher the kaolinite crystallinity, the more diffraction peaks will show up in the range of 19°–33° and 34°–40° and the peaks will be sharper and well

resolved (Noble 1971). Among them, diffraction peaks (110) and ($11\bar{1}$) are particularly sensitive to kaolinite crystallinity. Therefore, Hinckley (1963) proposed Hi to characterize the crystallinity of kaolinite.

Many studies have reported disordered stacking in kaolinite due to the relative shift between adjacent layers. This stacking behavior affords different polytypes of kaolinite. When the kaolinite layers are precisely stacked along the *c*-axis (zero shift), the O and OH groups of adjacent layers can be closely bonded to form hydrogen bonds. When the layers of kaolinite are translated or rotated relative to each other, O–OH pairs similar to zero shift can be generated (Bailey and Banfield 1995; Banfield et al. 1995; Barrios et al. 1977; Bookin et al. 1989; Brindley and Robinson 1946), wherein the polytype with a relatively stable structure is formed. Accordingly, previous studies proposed the following three stacking fault models for kaolinite: (1) stacking disorder due to displacements by $p\vec{b}/3$ (p is an integer) (Brindley 1980; Brindley and Robinson 1946; Giese 1982; Robert and Newnham 1961); (2) stacking disorder due to octahedral vacancy displacement (Plançon and Tchoubar 1977); (3) stacking disorder due to ±120° rotations (Murray 1954). They derived the computed XRD patterns from the stacking fault model to verify its validity. However, these stacking models do not accurately generate the calculated diffraction patterns that match the observed ones, where the ±120° model has been confirmed to be unrealistic (Artioli et al. 1995; Bookin et al. 1989).

Previous studies have proved that Hi is related to stacking order–disorder in kaolinite through infrared (Balan et al. 2005) and thermogravimetric–differential scanning calorimetry (TG–DCS) (Smykatz-Kloss 1974). However, these studies are mainly indirectly supported by the stretching vibration of OH groups between kaolinite layers or

This is the peer-reviewed, final accepted version for American Mineralogist, published by the Mineralogical Society of America.
The published version is subject to change. Cite as Authors (Year) Title. American Mineralogist, in press.
DOI: https://doi.org/10.2138/am-2022-8830. http://www.minsocam.org/

the energy to be overcome by dihydroxylation. There is currently no solid direct evidence for the relationship between OH groups and stacking order–disorder in kaolinite. Moreover, there is no agreement on the stacking order–disorder in kaolinite. On the one hand, when kaolinite is stacked at the zero shift, the hydrogen bonds between adjacent layers are closely bonded, which should belong to orderly stacking. Alternatively, the $p\vec{b}/3$ model has been reported as a weak stacking disorder in kaolinite (He et al. 2005; Robertson et al. 1954) and belongs to ordered stacking. A more precise determination of the stacking order–disorder in kaolinite is required. Therefore, accurately determining the stacking order–disorder in kaolinite is crucial and the primary focus of this study. The relation between Hi and the stacking order–disorder in kaolinite has been established herein.

High-quality kaolinite deposits of the world are mainly concentrated in China, the United States, Britain, Australia, and Brazil (Dewu and Durrance 1993; Murray and Keller 1993; Wilson et al. 2006). This study collected a series of kaolinite exhibiting different crystallinity from different origins worldwide. We simulated different stacking situations of kaolinite layers using first-principles calculation (Zhou et al. 2016), and the stacking order–disorder in kaolinite was defined by the difference in the lattice energy of stacking. Based on the defined stacking order–disorder in kaolinite, the crystallinity index of kaolinite was characterized via structural refinement. The new index (CIS) was found to be strongly correlated with Hi, indicating that Hi may be essentially related to stacking order–disorder in kaolinite.

Sample and Methods

Experimental and computational details

Herein, we collected six kaolinite samples of different origins and crystallinity from

China, the United States, and Australia and named them KL1–KL6 (KL for Kaolinite) in order of increased crystallinity. The samples were provided and purified by China Kaolinite Co., Ltd and Sinopec Changling Refining and Chemical Company. The samples were dried at 60℃ for 24 h and screened with a 200-mesh sieve to refine the sample particles and reduce the influence of sample size on the test results.

XRD data of the samples were collected using an X-ray diffractometer (D8 Advance, Bruker) equipped with a two-stage monochromator and a Cu radiation source (40 kV, 40 mA). As kaolinite is a layered clay mineral, and the conventional positive pressure method produces the preferred orientation, the scattering method is used in this study to remove the preferred orientation of the sample. The chemical component of the samples was characterized using an X-ray fluorescence spectrometer (AXIOS, Panalytical). A synchronous thermal analyzer was used to analyze the TG–DSC of the samples under the N_2 atmosphere, the temperature range was 30℃–1000℃, and the heating rate was 10℃/min. Fourier transform infrared spectrometer (PerkinElmer Spectrum100) was used to characterize the infrared spectrum of the samples. The mass ratio of KBr to kaolinite sample was 50:1, the measurement range was 4500–450 cm^{-1}, and 64 scans were performed. The samples were scanned using an atomic force microscope (AFM) equipped with a diamond probe at a scanning speed of 0.9 HZ and 256 scanning times.

The program TOPAS 5 (DIFFRAC.TOPAS Bruker version 5) was used for Rietveld refinement using the fundamental parameters method. The initial structural parameters of kaolinite were obtained from El-Sayed et al. (1990). The zero error, background, scale, peak profile, and lattice parameters of the phases were varied to achieve the best fit. The preferred orientation of (002) correction is based on March (1932). The background was

fitted by Cheary and Coelho (1992; 1994). Peak profiles were modeled using a Thompson–Cox–Hastings pseudo-Voigt function described by Young (1993). The kaolinite layers' stacking model was constructed using the "stacking faults" model in TOPAS 5. The refined kaolinite cell was used as the initial model, with the number of structure layers set to 22. Because the kaolinite structure layer is a rigid body that shifts freely in x, y, and z directions, the occupation of Si_2 was counted to represent the shift of the structural layer.

The lattice energies of different stackings were calculated with first-principles calculation in the Perdew–Burke–Ernzerhof (PBE)-type gradient generalized approximation (Perdew et al. 1996) using the projector augmented-wave method (Blöchl 1994) integrated into the Vienna ab initio simulation package (VASP) package (Kresse and Furthmüller 1996; Kresse and Joubert 1999). A series of stacking configurations with different relative shift vectors were set between two adjacent structure layers based on a 2 × 1 × 2 supercell of kaolinite along *a*, *b*, and *c* directions. The cutoff energy was 520 eV and the k-space was sampled with a mesh of 3 × 3 × 3 by the Monkhorst–Pack method.

Hinckley index (Hi)

Peaks (110) and (11$\bar{1}$) were selected as references to measure the heights (A and B) of diffraction peaks and the distance (B_t) from the peak of (110) to the dorsal bottom line (Figure 1). Hi is the ratio of the sum of A and B to B_t, with the following formula (Hinckley 1963).

$$Hi=\frac{A+B}{B_t} \quad (1)$$

Relative size estimation of $p\vec{b}$/3 stacking defect

$p\vec{b}$/3 can be estimated by the ratio of (020) to (11$\bar{1}$) diffraction peak intensity in the

This is the peer-reviewed, final accepted version for American Mineralogist, published by the Mineralogical Society of America.
The published version is subject to change. Cite as Authors (Year) Title. American Mineralogist, in press.
DOI: https://doi.org/10.2138/am-2022-8830. http://www.minsocam.org/

XRD pattern (Bailey 1985).

$$p\vec{b}/3 = \frac{I_{020}}{I_{11\bar{1}}} \quad (2)$$

Infrared crystallinity index (OI)

Kaolinite has two types of OH groups, inner surface OH groups and inner OH group, which are located at 3695, 3668, 3652 cm^{-1}, and 3620 cm^{-1} in the infrared absorption spectrum of kaolinite, respectively. Because the OH absorption band of the infrared spectrum of kaolinite in the high-frequency region is susceptible to the 1:1 stacking fault (Balan et al. 2005), the ratio of the intensity of two absorption bands, 3695 cm^{-1} and 3620 cm^{-1}, is often used to characterize the infrared crystallinity index of kaolinite–OI (Yang 1988).

$$OI = \frac{H_1}{H_2} \quad (3)$$

where H_1 represents the intensity of the absorption band 3704–3698 cm^{-1} (A1–OH stretching vibration band on the surface), and H_2 represents the intensity of the absorption peak 3628–3620 cm^{-1} (A1–OH stretching vibration band inside the octahedron).

RESULTS AND DISCUSSION

Crystal structure

Figure 2a shows the XRD patterns of kaolinite. The diffraction peaks of kaolinite are consistent with those in the Standard PDF card, indicating that kaolinite exhibits a pure phase. Figure 2b shows the XRD pattern of the diffraction zone (2θ = 19°–33°) of kaolinite (02*l*) and (11*l*). The Hi values of KL1–KL6 calculated according to Equation (1) are shown in Figure 2b. With an increase in the Hi value, the number of diffraction peaks of kaolinite increases and the peaks split well. In the XRD pattern of KL1, which has the lowest

This is the peer-reviewed, final accepted version for American Mineralogist, published by the Mineralogical Society of America.
The published version is subject to change. Cite as Authors (Year) Title. American Mineralogist, in press.
DOI: https://doi.org/10.2138/am-2022-8830. http://www.minsocam.org/

crystallinity in the sample, triple peaks { (020), ($1\bar{1}0$) and ($11\bar{1}$) } in the 19°–22° range are replaced by double peaks and the ($11\bar{1}$) reflection peaks are blurred. KL2–KL6 exhibit high crystallinity relative to KL1. More diffraction peaks and higher diffraction intensity are observed in the 19°–33° range. The reflection peak of (02*l*) and (11*l*) crystal band obviously splits as well as the reflection peaks of ($11\bar{1}$).

Table 1 lists the chemical components of kaolinite. The contents of SiO_2 and Al_2O_3, the main chemical component of kaolinite from different origins, are close to their theoretical values. Furthermore, the presence of only a small number of impurity elements, such as Fe, Ti, Ca, Mg, Na, and K, proved that kaolinite is almost pure.

Relation between stacking and Hi

The main interlayer force of kaolinite is hydrogen bonds (Yuan et al. 2013), and the relative translation of kaolinite layers can change the stacking state of the layers. Consequently, the relative positions of Si–O and Al–OH bonds between adjacent layers differ, the length and angle of the hydrogen bond change accordingly, and the vibrational properties of the OH groups on the inner surface change accordingly. Therefore, the infrared absorption spectrum of kaolinite can reflect its crystallinity to a certain extent.

Figure 3a shows the infrared absorption spectrum of kaolinite, and the low-frequency region of kaolinite is shown in Figure 3b. The absorption bands 1115, 1032, and 1001 cm^{-1} corresponded to the Si–O groups. The 913 cm^{-1} absorption band was attributed to the vibrational absorption of Al–OH in the octahedral sheet. The absorption bands located at 794 cm^{-1} and 754 cm^{-1} were assigned to the stretching vibration of Al–O–Si. The 696 cm^{-1} absorption band is due to the stretching vibration of Al–OH. There are two strong absorption bands in the range of 550–450 cm^{-1}, in which 537 cm^{-1} was mainly attributed

to the stretching vibration of Si–O–Al, while 465 cm^{-1} was attributed to the stretching vibration of Si–O. Four OH absorption bands exist in the high-frequency region of 3600–3700, 3695, 3668, 3652 (inner surface OH groups), and 3620 cm^{-1} (inner OH group). As the crystallinity of kaolinite decreases, the internal structure arrangement becomes irregular, and the symmetry decreases. In the infrared absorption spectrum, the absorption band is widened, and the absorption intensity of the spectral band is reduced (Cruz-Cumplido et al. 1982). Figure 3c shows that the intensities of the 3668 cm^{-1} and 3652 cm^{-1} absorption bands of KL1 are extremely low, and the absorption bands are widened, indicating its disordered crystallization. As the crystallinity of kaolinite increases, the peak patterns of 3695 cm^{-1} and 3620 cm^{-1} absorption bands gradually become sharp. The larger the ratio, the higher the crystallinity. The fitting of the OI index from the ratio of the intensity of two absorption bands and Hi (Figure 3d) shows that the OI index is positively correlated with Hi, indicating that the OH absorption band between kaolinite layers can reflect the crystallinity of kaolinite to a certain extent.

Additionally, kaolinite can be dehydroxylated into metakaolinite under heat treatment, and its dehydroxylation temperature increases as kaolinite crystallinity increases (Smykatz-Kloss 1974). Figure 4a–f shows the TG–DSC analysis of kaolinite. The endothermic valley at about 176℃ can be observed in Figure 4, and its TG curve also shows a weight decrease at this temperature due to the loss of adsorption water of kaolinite. Between 400℃ and 700℃, a sharp decline can be observed in the TG curve of kaolinite, and there is a strong endothermic valley between 505℃ and 530℃. This is due to the gradual removal of interlayer crystalline water of kaolinite, and the layered structure of kaolinite was gradually destroyed and transformed into amorphous metakaolinite.

Smykatz-Kloss (1974) highlighted that the dehydroxylation temperature of kaolinite was related to its crystallinity: the higher the crystallinity, the higher the dehydroxylation temperature. It is generally believed that when Hi > 1, kaolinite crystallizes well, and the dehydroxylation temperature of kaolinite exceeds 525℃. When Hi < 1, kaolinite crystallizes poorly, and the dehydroxylation temperature of kaolinite decreases to about 500℃ (Figure 5a). In essence, different stacking states will lead to the change of hydrogen bond strength, which will lead to the different heat absorption energy of dehydroxylation, so the dehydroxylation temperature of kaolinite will change with Hi.

The analysis of infrared and TG–DSC of kaolinite can indirectly indicate that Hi may be related to the stacking order–disorder in kaolinite. However, the interlayer forces of kaolinite are derived from hydrogen bonds between tetrahedral sheets and adjacent octahedra sheets and include van der Waals forces and electrostatic forces. Thus, the OI index mainly reflects the vibration state of the OH group. At the same time, kaolinite dehydroxylation mainly overcomes the interlayer hydrogen bond energy and the covalent bond energy between Al–OH, both of which are difficult to reflect the genuine relation between interlayer force and crystallinity. Therefore, although the experimental results of infrared and TG–DSC have a specific correlation with Hi, it can be indirectly proven that Hi may be related to the stacking order–disorder in kaolinite, but there is no more direct evidence.

Therefore, to obtain more direct evidence, we used AFM to count the average thickness of kaolinite and fit it to Hi. Figure 5b shows the correlation between the stacking thickness of kaolinite and Hi. The Hi value positively correlates with the stacking thickness and is highly fitted (R^2 = 0.902). The average stacking thickness of kaolinite increased

from 22 to 76 nm as the Hi value increased. When kaolinite crystallinity is poor, the stacking is relatively disordered, and the lattice energy of layer stacking is high, which leads to the thin thickness of layer stacking. With the stronger crystallinity of kaolinite, stacking becomes orderly, and the lattice energy of layer stacking decreases so that the stacking of kaolinite is easier to grow thick (De and Navrotsky 1999; Zhang et al. 2021a).

In conclusion, the stacking order–disorder in kaolinite will directly affect its lattice energy. When the stacking of kaolinite is orderly, the lattice energy decreases, the crystal thickness increases, and the Hi value increases. Therefore, it can be inferred that Hi is directly affected by the stacking order–disorder in kaolinite.

Determination of stacking order–disorder in kaolinite

To determine the stacking order–disorder of the kaolinite layer, a series of kaolinite supercell structures with different stacking states were constructed by relative translation of two adjacent layers, and the lattice energy was calculated using first-principles simulation. Kaolinite is a typical 1:1 clay mineral, in which layers are held together by hydrogen bonds either than dispersive interaction. It has been found that the inclusion of dispersive interaction can improve the prediction of unit cell volumes and cell parameters (Tunega et al. 2012). However, the improvement is not so significant like talc and pyrophyllite, in which dispersion force is very important. Meanwhile, the dispersive interaction corrections lead to a significant underestimation of the length of the vector c of kaolinite, the deviations are even more than the overestimation of the length of the vector c in the standard PBE method. As cell parameter c is one of the most important indices for kaolinite, so it is hard to say the dispersive interaction corrections can bring positive profit. The calculations including dispersive interactions based on PBE-D2 (Grimme 2006) and

This is the peer-reviewed, final accepted version for American Mineralogist, published by the Mineralogical Society of America.
The published version is subject to change. Cite as Authors (Year) Title. American Mineralogist, in press.
DOI: https://doi.org/10.2138/am-2022-8830. http://www.minsocam.org/

vdW-TS (Tkatchenko and Scheffler 2009) approaches have been tested for several configurations. The results show that the lattice energies change a lot compared to that performed based on the standard PBE method with no dispersive interactions, but the lowest configuration is not changed. Furthermore, the DFT calculations are only a very small part of this study, which aims to determine the ordered shift type. Usually, vibrational and configurational entropy corrections should not be ignored under finite temperatures although they are occupied only a very small percentage of free energy. But this study is not a detailed thermodynamical computational study, so the lack of vibrational and configurational entropy corrections does not affect the main viewpoints of this study. Because DFT calculations with standard PBE functional also can provide relatively good accuracy for hydrogen bonds (Tunega et al. 2012), and also considering the computational cost, all the calculations in this study used this scheme without dispersive interactions, vibrational and configurational entropy corrections.

Figure 6a shows several characteristic stacking states of kaolinite. The position of the initial layer is fixed. ① shows the second layer translates n$\vec{a}$ along $\vec{a}$ relative to the initial layer or does not translate, where n is an integer (Figure 6a). Conversely, ④ indicates the second layer translates $\frac{\sqrt{3}}{3}$b relative to the initial layer along the direction of 30/150° with respect to $\vec{b}$ (Figure 6a). In these two stacking states, the projections of two adjacent layers in the $\vec{c}$ direction coincide (Figure 6b), which are equivalent structures and are denoted as zero shift. In Figure 6a, ② and ③ are stacking translations along $\vec{b}$ at p$\vec{b}$/3 (Figure 6c, Table 1), respectively. We constructed an approximate potential energy surface of kaolinite in plane *a*–*b* (the surface parallel to (001)) from the lattice energy of the different stacking

This is the peer-reviewed, final accepted version for American Mineralogist, published by the Mineralogical Society of America.
The published version is subject to change. Cite as Authors (Year) Title. American Mineralogist, in press.
DOI: https://doi.org/10.2138/am-2022-8830. http://www.minsocam.org/

states of kaolinite (Figure 7). Si2 (★) in the initial layer is set as the origin, and the second layer is translated relative to the origin. The coordinates in Figure 7 show the occupying position in Si2 in the second layer. It can be observed from Figure 7 that zero shift stacking has the lowest energy, and the occupying position can form a hexagonal lattice, which according to the crystal structure characteristics of kaolinite, should be identified as ordered stacking. The p$\vec{b}$/3 stacking defect has the second lowest energy. However, the amount of p$\vec{b}$/3 stacking defect gradually increases with decreased Hi value (Table 1), so it should be identified as disordered stacking. The lattice energy of other stacking states is higher than that of these two stacking states, so they all belong to disordered stacking.

Analysis of the CIS

To relate Hi to the stacking order–disorder in kaolinite, we propose a crystallinity index based on the stacking (CIS) order–disorder in kaolinite. Mathematical fitting of CIS and Hi can reflect the relation between Hi and the stacking order–disorder in kaolinite. Kübler (1967) defined crystallinity as the degree of order in a crystalline substance lattice. From the perspective of stacking order–disorder, kaolinite crystallinity should be the proportion of the ordered stacking number in the total stacking number. Therefore, we define zero shift as ordered stacking, and its proportion in the total stacking number represents the CIS (Equation 4).

$$\mathrm{CIS}=\frac{N_{OS}}{N_S}=\frac{N_{0d}}{N_S} \quad (4)$$

where N_{OS} represents the number of ordered stacking, N_S represents the total stacking, and N_{0d} represents the number of zero shift stacking.

According to the stacking lattice energy obtained by simulation calculation, the stacking energy of zero shift is the lowest, and the lattice energy is the same when the

relative position difference is <0.1 Å (displacement of the projection of Si2 on two adjacent layers on *a*–*b* plane) with zero shift stacking. Therefore, zero shift stacking (<0.1 Å) can be used as orderly stacking. According to the definition of the CIS, we first need to obtain parameters of N_{OS} and N_S, which can be obtained from XRD data by structural refinement. Structure refinement is a method of resolving crystal structure by fitting the XRD patterns using the least square method (Young et al. 1977). The structure information of kaolinite stacking can be obtained using a supercell for structural refinement (Cockayne et al. 2021). Therefore, the structure refinement method can be used to fit a series of XRD data of kaolinite with different crystallinity by supercell. Subsequently, the stacking state of the kaolinite layer can be obtained.

When kaolinite crystallizes well, the number of diffraction peaks increases and the peaks become sharper, narrower, and more symmetrical (Agyei-Tuffour et al. 2014; Chen et al. 2004; Frost et al. 2002). As kaolinite crystallinity decreases, gentle hump-like peaks appear, as some diffraction peaks may not be resolved (Li et al. 2019; Sánchez-Soto et al. 2000). Therefore, there is often a significant error in the structure refinement of kaolinite with low crystallinity (Paz et al. 2018). When the number of layers of the constructed supercell is large enough, the structure information of kaolinite will be obtained, and the error of the structure refinement will be reduced. However, with the increase of stacking layers of supercells, the computation amount of structure refinement also increases exponentially, and the time cost of structure refinement also increases significantly. Therefore, the structural refinement method calculated the diffraction pattern of KL1 (with the lowest crystallinity), and the changes of CIS values were simulated under the stacking number of 5–25 layers and repeated three times, respectively, to select the optimal number

This is the peer-reviewed, final accepted version for American Mineralogist, published by the Mineralogical Society of America.
The published version is subject to change. Cite as Authors (Year) Title. American Mineralogist, in press.
DOI: https://doi.org/10.2138/am-2022-8830. http://www.minsocam.org/

of supercell layers for structural refinement. Figure 8 shows the influence of structural refinement of different layers of kaolinite supercell on the CIS (average value). When the number of stacking layers is small, the CIS fluctuates sharply with increased stacking layers. At this stage, the standard deviation of repeated structure refinement is considerable. When the number of stacking layers further increases, the fluctuation flattens, and the standard deviation gradually decreases. It indicates that increasing the number of stacking layers of the structure refinement can improve the repeatability and stability of the data. The CIS tends to be balanced until the number of stacking layers is 22. Therefore, we used kaolinite supercells of 22 stacking layers to refine the structure of KL1–6 to obtain the structure information of the stacking of kaolinite layers.

CIS

Figure 9a–f shows the projection of the layer translation of kaolinite on *a*–*b* plane. We counted the projection of Si2 in each layer on *a*–*b* plane, representing the translation of each layer on *a*–*b* plane. Furthermore, 1–22 represents the number of stacking layers, the first layer is the initial layer, and the remaining 21 layers are translated freely within the range of supercell. When the kaolinite crystallinity is low (Figure 9a–b), the number of characteristic translations is small, and most of them are irregular translations, indicating that the stacking is very disordered. When the crystallinity gradually increased (Figure 9c–e), the number of ① and ④ type translations (Figure 6a) gradually increased, and the number of ordered stacking in the supercell gradually increased. When the crystallinity is further increased (Figure 9f), the translation of layer in supercell is mostly of type ① (Figure 6a), and the number of ordered stacking increases further.

According to the stacking state of kaolinite in Figure 9a–f, we counted its CIS, fitted

it against Hi, and found that the fitting was excellent, with an R^2 as high as 0.979. The CIS and Hi correlate well in mathematics, indicating that their physical meanings are similar. Therefore, Hi can be used to reflect the degree of ordering in kaolinite stacking. We repeated the CIS six times to verify its repeatability of CIS and averaged the repeated structural refinement data in 2–6 groups (Figure 10a). The CIS and Hi's fitting reached an $R^2 = 0.986$ when the average of four repeated structural refinements was taken (Figure 10b). However, more repeated structural refinement did not bring considerable improvement. Therefore, performing at least four repeated structural refinements when using CIS to characterize kaolinite crystallinity is necessary.

IMPLICATIONS

Characterizing the crystallinity index of kaolinite using Hi is simple and feasible. Thus, Hi is widely used in the industry to investigate the physical and chemical properties of kaolinite. Through infrared (Balan et al. 2005) and TG–DSC (Smykatz-Kloss 1974), it can be inferred that Hi may be related to the stacking order–disorder in kaolinite; however, there is no direct evidence to prove this thus far. Additionally, there is no agreement on the classification of the stacking order–disorder in kaolinite.

Herein, the lattice energy of kaolinite with different stacking states was calculated using first-principles simulation. The lattice energy of ordered stacking was the lowest. Thus, it is inferred that only the zero shift stacking is ordered, and the rest are disordered stacking. Utilizing structure refinement, supercells of 22 stacking layers were constructed to fit the XRD pattern of kaolinite, and the stacking state of kaolinite was simulated. A new CIS crystallinity index was established by dividing the order–disorder of stacking. The CIS has good repeatability and fits well with Hi; thus, it can supplement Hi, particularly for

kaolinite with low crystallinity. Further, direct evidence of the order–disorder correlation between Hi and the stacking of kaolinite layers is presented for the first time. On this basis, modifying kaolinite to adjust its crystallinity has theoretical guidance. The industrial application of kaolinite with different crystallinity due to different origins is no longer limited. Therefore, this paper is important for efficiently utilizing kaolinite resources.

ACKNOWLEDGEMENTS AND FUNDING

This study is supported by the National Natural Science Foundation of China (42072053).

REFERENCES CITED

Agyei-Tuffour, B., Bensah, Y.D., Damoah, L.N.W., Dodoo-Arhin, D., Yaya, A., Nyankson, E., Annan E., Sarkodee E., Efavi, J.K. (2014). Synthesis and microstructural characterization of kaolin–polyethylene composites. Polymer composites, 35(8), 1507-1515.

Amigó, J.M., Bastida, J., Sanz, A., and Signes, M. (1994) Crystallinity of lower cretaceous kaolinites of teruel (spain). Applied Clay Science, 9(1), 51-69.

Ahmad, S. (2020). Acoustic and thermal insulation of nanocomposites for building material: improvement of sound and thermal insulation properties of nanocomposite. Baghdad Science Journal, 17(2), 494-501.

Aparicio, P., Galán, E., and Ferrell, R.E. (2006). A new kaolinite order index based on XRD profile fitting. Clay Minerals, 41(4), 811-817.

Artioli, G., Bellotto, M., Gualtieri, A., and Pavese, A. (1995). Nature of structural disorder in natural kaolinites: a new model based on computer simulation of powder diffraction data and electrostatic energy calculation. Clays and Clay Minerals, 43(4), 438-445.

Bailey, S.W., and Banfield, J.F. (1995). Derivation and identification of nonstandard

serpentine polytypes. American Mineralogist, 80(11-12), 1104-1115.

Bailey, S.W. (1985). Structural studies of clay minerals during 1981–1985, in "Proceedings of the International Clay Conference, Denver, 1985", L.g. Schultz, H. van Olphen and F.A. Mumpton, eds., Clay Minerals Society, Bloomington.

Balan, E., Lazzeri, M., Saitta, A.M., Allard, T., Fuchs, Y., and Mauri, F. (2005). First-principles study of OH-stretching modes in kaolinite, dickite, and nacrite. American Mineralogist, 90(1), 50-60.

Banfield, J.F., Bailey, S.W., Barker, W.W., and Smith, R.C. (1995). Complex polytypism: Relationships between serpentine structural characteristics and deformation. American Mineralogist, 80(11-12), 1116-1131.

Barrios, J., Plançon, A., Cruz, M. I., and Tchoubar, C. (1977). Qualitative and quantitative study of stacking faults in a hydrazine treated kaolinite—relationship with the infrared spectra. Clays and Clay Minerals, 25(6), 422-429.

Bergaya, F., and Lagaly, G. (2013). Handbook of clay science. Newnes.

Blöchl, P.E. (1994). Projector augmented-wave method. Physical Review B, 50(24), 17953.

Bookin, A.S., Drits, V.A., Plancon, A., and Tchoubar, C. (1989). Stacking faults in kaolin-group minerals in the light of real structural features. Clays and Clay Minerals, 37(4), 297-307.

Brindley, G.W. (1980). Crystal structures of clay minerals of clay minerals and their x-ray identification. Earth Science Reviews, 18(1), 84-85.

Brindley, G.W, and Robinson, K. (1946). Randomness in the structures of kaolinitic clay minerals. Transactions of the Faraday Society, 42, B198-B205.

Cheary, R.W., and Coelho, A. (1992). A fundamental parameters approach to X-ray line-

profile fitting. Journal of Applied Crystallography, 25(2), 109-121.

Cheary, R.W., and Coelho, A. (1994). Synthesizing and fitting linear position-sensitive detector step-scanned line profiles. Journal of applied crystallography, 27(5), 673-681.

Chen, Y.F., Wang, M.C., and Hon, M.H. (2004). Phase transformation and growth of mullite in kaolin ceramics. Journal of the European Ceramic Society, 24(8), 2389-2397.

Cheng, H.F., She, G., and Zhou, Y. (2018). Study on the chargeability of kaolinite with different crystallinity. Journal of Synthetic Crystals, 47(9), 1910-1916.

Cockayne, E., Wong-Ng, W., Chen, Y.S., Culp, J.T., and Allen, A.J. (2021). Density Functional Theory Study of the Structure of the Pillared Hofmann Compound Ni (3-Methyl-4, 4′-bipyridine) [$Ni(CN)_4$] (Ni-BpyMe or PICNIC-21). The Journal of Physical Chemistry C, 125(29), 15882-15889.

Cruz-Cumplido, M., Sow, C., and Fripiat, J.J. (1982). Spectre infrarouge des hydroxyles, cristallinité et énergie de cohésion des kaolins. Bulletin de Minéralogie, 105(5), 493-498.

De Ligny, D., and Navrotsky, A. (1999). Energetics of kaolin polymorphs. American Mineralogist, 84(4), 506-516.

Dewu, B.B.M., and Durrance, E.M. (1993). Mobility of U and granite kaolinization in southwest England. In: Murray HH, Bundy WM, Harvey CC (eds) Kaolin Genesis and Utilization. The Clay Minerals Society Sp Publ 1: 205-219.

El-Sayed, K., Heiba, Z.K., and Abdel-Rahman, A.M. (1990). Crystal structure analysis and refinement of Kalabsha kaolinite ($Al_2Si_2O_5(OH)_4$). Crystal Research and Technology, 25(3), 305-312.

Fernandez, R., Martirena, F., and Scrivener, K.L. (2011). The origin of the pozzolanic activity of calcined clay minerals: A comparison between kaolinite, illite and montmorillonite. Cement and concrete research, 41(1), 113-122.

Frost, R.L., Van Der Gaast, S.J., Zbik, M., Kloprogge, J.T., and Paroz, G. N. (2002). Birdwood kaolinite: a highly ordered kaolinite that is difficult to intercalate—an XRD, SEM and Raman spectroscopic study. Applied Clay Science, 20(4-5), 177-187.

Giese, R.F. (1982). Theoretical studies of the kaolin minerals; electrostatic calculations. Bulletin de Mineralogie, 105(5), 417-424.

Grimme, S. (2006). Semiempirical GGA-type density functional constructed with a long-range dispersion correction. Journal of computational chemistry, 27(15), 1787-1799.

Gu, X., Wang, Y., Liu, X., Zhang, S., Li, H., Sun, J., and Tang, W. (2020). Efficient approach to enhancing the fire resistance of polypropylene by modified microporous aluminosilicate from kaolinite as synergist. Polymers for Advanced Technologies, 31(5), 1047-1058.

Guo, R., Yao, W., Ma, H., and Yuan, J. (2020). Two-step hydrothermal synthesis of nano-kaolinite from fly ash: Thermodynamics and mechanism. Journal of Cleaner Production, 271, 122567.

Hammas, A., Lecomte-Nana, G., Daou, I., Tessier-Doyen, N., Peyratout, C., and Zibouche, F. (2020). Kaolinite-Magnesite or Kaolinite–Talc-Based Ceramics. Part II: Microstructure and the Final Properties Related Sintered Tapes. Minerals, 10(12), 1080.

He, H., Yuan, P., Guo, J., Zhu, J., and Hu, C. (2005). The influence of random defect density on the thermal stability of kaolinites. Journal of the American Ceramic Society, 88(4),

1017-1019.

Hinckley, D.N. (1963). Variability in "crystallinity" values among the kaolin deposits of the coastal plain of georgia and south carolina. Clays and Clay Minerals, 11(1), 229-235.

Hughes, J.C, and Brown, G. (2010) A crystallinity index for soil kaolins and its relation to parent rock, climate and soil maturity. European Journal of Soil Science, 30(3), 557-563.

Indahwati, E., Af'idah, N., and Wati, D.A.R. (2020). Pengaruh penambahan kaolinite lokal kabupaten jombang pada refractory bricks terhadap karakteristik mekanis. Sainsteknopak, 4(1), 123-127.

Kresse, G., and Furthmüller, J. (1996). Efficient iterative schemes for ab initio total energy calculations using a plane-wave basis set. Physical Review B, 54(16), 11169.

Kresse, G., and Joubert, D. (1999). From ultrasoft pseudopotentials to the projector augmented-wave method. Physical Review B, 59(3), 1758.

Kogure, T. (2011). Stacking disorder in kaolinite revealed by HRTEM: a review. Clay science, 15(1), p.3-11.

Kübler, B. (1967). La cristallinité de l'illite et les zones tout áfait supécieures du métamorphisme. In Étages Tectoniques. Collogue de Neuchâtel 1996, pp. 105-121.

Li, J., Zuo, X., Zhao, X., Ouyang, J., and Yang, H. (2019). Insight into the effect of crystallographic structure on thermal conductivity of kaolinite nanoclay. Applied Clay Science, 173, 12-18.

Liétard, O. (1977) Contribution à l'étude des propriétés physicochimiques, cristallographiques et morphologiques des kaolins. Thèse unique, Institut National

Polytechnique de Lorraine, Nancy, France. 322.

Liu X.Y., Yuan C.Y., Gao X.H., and Zhang L. (2020). Synthesis of pseudo-boehmite@kaolinite composite and its application in FCC catalyst. Petrochemical Technology, 49(3), 219.

Liu, Y., Huang, Q., Zhao, L., and Lei, S. (2021). Influence of kaolinite crystallinity and calcination conditions on the pozzolanic activity of metakaolin. Gospodarka Surowcami Mineralnymi-Mineral Resources Management, 37(1), 39-56.

Ma, C., and Eggleton, R.A. (1999). Surface layer types of kaolinite: a high-resolution transmission electron microscope study. Clays and Clay Minerals, 47(2), 181-191.

March, A. (1932). Mathematische Theorie der Regelung nach der Korngestalt bei affiner Deformation: Zeitschrift fur Kristallographie, 81, 285-297.

Murray, H.H. (1954). Structural variations of some kaolinites in relation to dehydrated halloysite. American Mineralogist, 39(1-2), 97–108.

Murray, H.H., and Keller, W.D. (1993). Kaolins, kaolins and kaolins. In: Murray, H., Bundy, W., Harvey, C. (Eds.), Kaolin: Genesis and utilization. Clay Minerals Society, Boulder, Colorado, pp. 1–24.

Murray, H.H. and Lyons, S.C. (1960). Further correlations of kaolinite crystallinity with chemical and physical properties. Clays and Clay Minerals, 8, 11-17.

Noble, F.R. (1971). A study of disorder in kaolinite. Clay minerals, 9(1), 71-81.

Pauling, L. (1930). The structure of the chlorites. Proceedings of the National Academy of Sciences, 16(9), 578-582.

Paz, S.P.A.D., Kahn, H., and Angélica, R.S. (2018). A proposal for bauxite quality control using the combined Rietveld–Le Bail–Internal Standard PXRD Method–Part 1: *hkl*

model developed for kaolinite. Minerals Engineering, 118, 52-61.

Perdew, J.P., Burke, K., and Ernzerhof, M. (1996). Generalized gradient approximation made simple. Physical Review Letters, 77(18), 3865.

Plançon, A., and Tchoubar, C. (1977). Determination of structural defects in phyllosilicates by X-ray powder diffraction—II. Nature and proportion of defects in natural kaolinites. Clays and Clay Minerals, 25(6), 436-450.

Plançon, A., and Zacharie, C. (1990). An expert system for the structural characterization of kaolinites. Clay Minerals, 25(3), 249-260.

Qin, L., Zhang, Y., Zhang, Y., and Gong, Y. (2021). Efficient preparation of coal-series kaolinite intercalation compounds via a catalytic method and their reinforcement for styrene butadiene rubber composite. Applied Clay Science, 213, 106237.

Range, K.J. and Weiss, A. (1969) Über das Verhalten von Kaoliniti bei hohen Drücken. Berichte der Deutschen Keramischen Gesellschaft, 46, 231–288.

Robert, E., and Newnham, M.S. (1961). A refinement of the dickite structure and some remarks on polymorphism in kaolin minerals. Mineralogical Magazine, 32, 683-704.

Robertson, R.H.S., Brindley, G.W., and Mackenzie, R.C. (1954). Mineralogy of kaolin clays from Pugu, Tanganyika. American Mineralogist: Journal of Earth and Planetary Materials, 39(1-2), 118-138.

Sánchez-Soto, P.J., del Carmen Jiménez de Haro, M., Pérez-Maqueda, L.A., Varona, I., and Pérez-Rodríguez, J.L. (2000). Effects of dry grinding on the structural changes of kaolinite powders. Journal of the American Ceramic Society, 83(7), 1649-1657.

Smykatz-Kloss, W. (1974) Differential Thermal Analysis: Application and Results in Mineralogy. Springer-Verlag, Heidelberg-Berlin, New York.

Stoch, L. (1974). Minerały ilaste, Wyd. Geologiczne, Warszawa, 172-174.

Tkatchenko, A. and Scheffler, M. (2009). Accurate molecular van der Waals interactions from ground-state electron density and free-atom reference data. Physical review letters, 102(7), 073005.

Tunega, D., Bučko, T., Zaoui, A. (2012). Assessment of ten DFT methods in predicting structures of sheet silicates: Importance of dispersion corrections. The Journal of chemical physics, 137(11), 114105.

Whittaker, H. (1939). Effect of particle size on plasticity of kaolinite. Journal of the American Ceramic Society, 22(1-12), 16-23.

Więckowski, T., and Wiewióra, A. (1976). New approach to the problem of the interlayer bonding in kaolinite. Clays and Clay Minerals, 24(5), 219-223.

Wilson, I.R., de Souza Santos, H., and de Souza Santos, P. (2006). Kaolin and halloysite deposits of Brazil. Clay minerals, 41(3), 697-716.

Yang, Z. (1988). Infra-red spectra analysis for clay minerals of kaolinites. Petroleum Geology and Expeximent, (01), 63-69.

Young, R.A. (1993). The Rietveld Method, edited by R.A. Young, IUCr Book Series, Oxford University Press 1993, 1-39.

Young, R.A., Mackie, P.T., and Von Dreele, R.B. (1977). Application of the pattern-fitting structure-refinement method of X-ray powder diffractometer patterns. Journal of Applied Crystallography, 10(4), 262-269.

Yuan, P., Tan, D., Annabi-Bergaya, F., Yan, W., Liu, D., and Liu, Z. (2013). From platy kaolinite to aluminosilicate nanoroll via one-step delamination of kaolinite: effect of the temperature of intercalation. Applied Clay Science, 83, 68-76.

Zadvernyuk, H., Kadoshnikov, V., Shekhunova, S., and Remez, S. (2021). Particle size distribution and crystallinity as indicators of kaolinite genesis. Applied Clay Science, 213, 106236.

Zhang, H., Zhang, Y., Lei, D., and Jiao, Y. (2021a). Characterization of structure of kaolinite in tectonically deformed coal: evidence of mechanochemistry. Energy Sources, Part A: Recovery, Utilization, and Environmental Effects, 5, 1-12.

Zhang, S., Gao, N., and Liu, K. (2021b). Insights on the intercalation mechanism of the coal-bearing kaolinite intercalation based on experimental investigation and molecular dynamics simulations. Chemical Papers, 75(12), 6335-6344.

Zhou, G., and Ling, Y. (1991). The crystallinity of kaolinite and its effect on the viscosity concentration of paper coating. Acta Mineralogica Sinica, 11(3), 7.

Zhou, J., Lu, X., and Boek, E.S. (2016). Changes in the interlayer structure and thermodynamics of hydrated montmorillonite under basin conditions: Molecular simulation approaches. Clays and Clay Minerals, 64(4), 503-511.

LIST OF FIGURE CAPTIONS

FIGURE 1. Illustration of the calculation of Hi. The diffraction pattern is fragment of KL6 with high crystallinity and clear diffraction peak.

FIGURE 2. X-ray diffraction (XRD) patterns of kaolinite (a), 19°–33° region of the XRD pattern of kaolinite, which is very sensitive to changes in crystallinity (b).

FIGURE 3. Infrared spectrum of KL1–KL6 (a), low-frequency region of the infrared spectrum, where the major groups of kaolinite are labeled (b), high-frequency OH region of the infrared spectrum, which is sensitive to the change of crystallinity of kaolinite (c), the relation between Hi and OI index (d).

FIGURE 4. TG–DSC analysis of KL1–KL6 (a–f). It is mainly used to characterize the dehydroxylation temperature of kaolinite, which is affected by the crystallinity of kaolinite.

FIGURE 5. The relation between Hi and dehydroxylation temperature of samples (the values were obtained from the DSC) (a) and layer-stacking thickness of samples (the values were obtained from the AFM) in relation with Hi (b).

FIGURE 6. Characteristic stacking states of kaolinite, the first layer does not move, and the second layer slides according to the marks in the figure (a), zero shift stacking marked with ①④ (b), $p\vec{b}/3$ stacking marked with ②③ (c).

FIGURE 7. Potential energy surface of kaolinite under different stacking states. The more ordered the stacking, the lower the lattice energy. Therefore, ordered stacking can be obtained by characterizing the lattice energy of stacking.

FIGURE 8. Effect of stacking layers on the CIS to find the optimal number of layers for structure refinement.

FIGURE 9. Projection of each kaolinite layer on plane *a*–*b* to visualize the displacement of the layers, KL1–KL6 (a–f), and a fitting plot of CIS against Hi to prove that Hi is mainly affected by the stacking order–disorder in kaolinite (g).

FIGURE 10. Influence of times of structure refinement on the correlation between Hi and CIS (a), and a linear fitting of CIS (the average of four repeated structural refinements) against Hi (b).

This is the peer-reviewed, final accepted version for American Mineralogist, published by the Mineralogical Society of America.
The published version is subject to change. Cite as Authors (Year) Title. American Mineralogist, in press.
DOI: https://doi.org/10.2138/am-2022-8830. http://www.minsocam.org/

TABLES

TABLE 1. Quantitative estimation of chemical component (wt%) and structural defects of kaolinite

sample number	KL1	KL2	KL3	KL4	KL5	KL6	theoretical values
origin	China	China	China	America	Australia	Australia	-
SiO_2	51.18	53.97	50.46	56.81	54.78	51.08	54.09
Al_2O_3	46.39	43.88	47.3	40.55	44.2	48.17	45.91
Fe_2O_3	1.13	0.97	0.12	0.82	0.2	0.12	-
TiO_2	0.08	0.07	0.09	1.17	0.26	0.21	-
CaO	0.03	0.02	0.09	0.04	0.01	-	-
MgO	0.06	0.05	0.04	0.05	0.05	0.05	-
Na_2O	0.05	0.02	-	0.13	0.04	-	-
K_2O	0.37	0.69	0.31	0.2	0.35	0.29	-
Hi	0.04	0.51	0.76	0.83	1.11	1.17	-
$p\vec{b}/3$	1.33	1.23	0.96	0.82	0.81	0.68	-

[#] The theoretical value of the chemical component of kaolinite is calculated by its molecular formula. The structural water content in the theoretical value is removed to better compare with the experimental characterization data of kaolinite.

This is the peer-reviewed, final accepted version for American Mineralogist, published by the Mineralogical Society of America.
The published version is subject to change. Cite as Authors (Year) Title. American Mineralogist, in press.
DOI: https://doi.org/10.2138/am-2022-8830. http://www.minsocam.org/

FIGURES

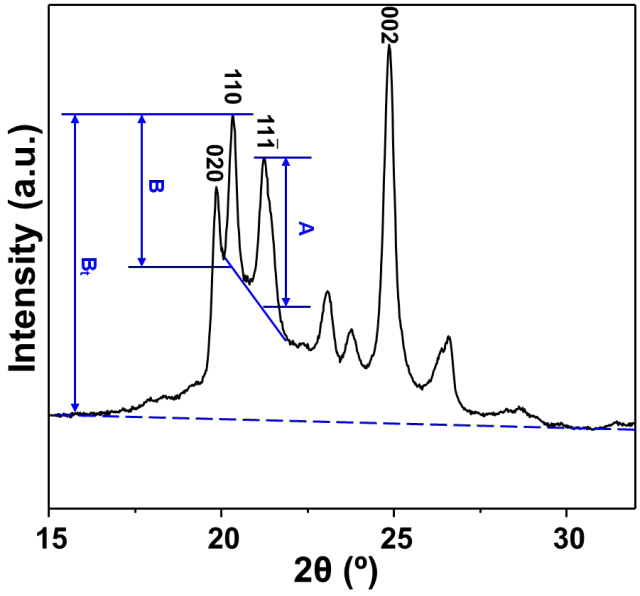

FIGURE 1. Illustration of the calculation of Hi. The diffraction pattern is fragment of KL6 with high crystallinity and clear diffraction peaks.

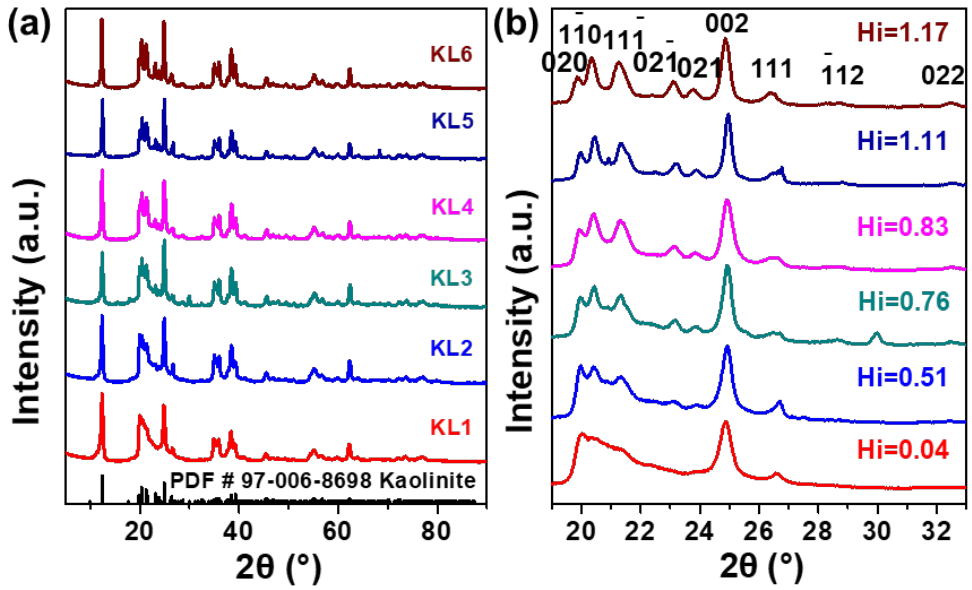

FIGURE 2. X-ray diffraction (XRD) patterns of kaolinite (a), 19°–33° region of the XRD pattern of kaolinite, which is very sensitive to changes in crystallinity (b).

This is the peer-reviewed, final accepted version for American Mineralogist, published by the Mineralogical Society of America.
The published version is subject to change. Cite as Authors (Year) Title. American Mineralogist, in press.
DOI: https://doi.org/10.2138/am-2022-8830. http://www.minsocam.org/

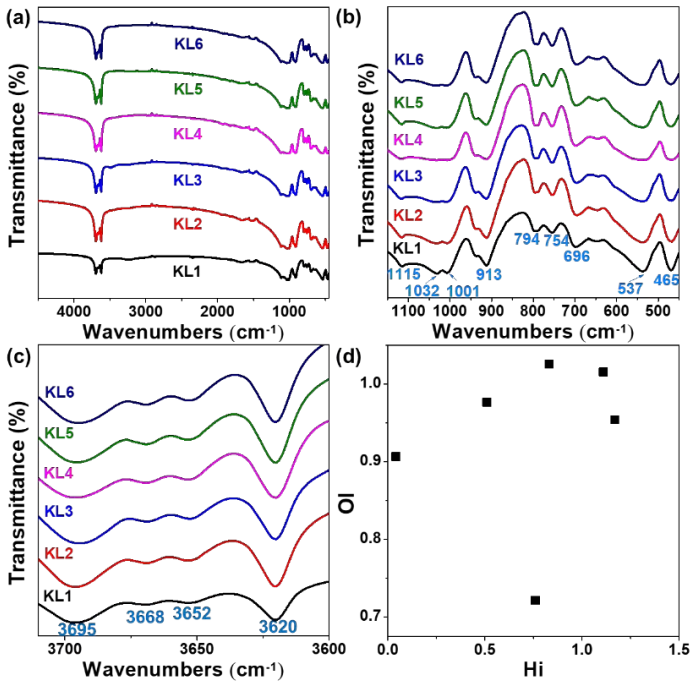

FIGURE 3. Infrared spectrum of KL1–KL6 (a), low-frequency region of the infrared spectrum, where the major groups of kaolinite are labeled (b), high-frequency OH region of the infrared spectrum, which is sensitive to the change of crystallinity of kaolinite (c), the relation between Hi and OI index (d).

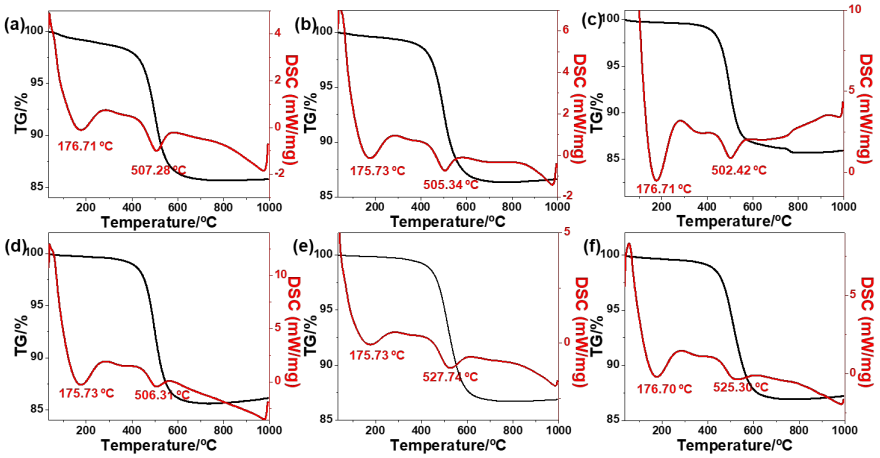

FIGURE 4. TG–DSC analysis of KL1–KL6 (a–f). It is mainly used to characterize the dehydroxylation temperature of kaolinite, which is affected by the crystallinity of kaolinite.

This is the peer-reviewed, final accepted version for American Mineralogist, published by the Mineralogical Society of America.
The published version is subject to change. Cite as Authors (Year) Title. American Mineralogist, in press.
DOI: https://doi.org/10.2138/am-2022-8830. http://www.minsocam.org/

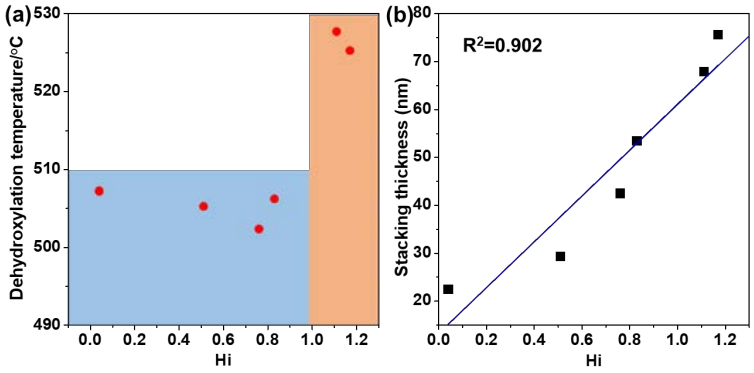

FIGURE 5. The relation between Hi and dehydroxylation temperature of samples (the values were obtained from the DSC) (a) and layer-stacking thickness of samples (the values were obtained from the AFM) in relation with Hi (b).

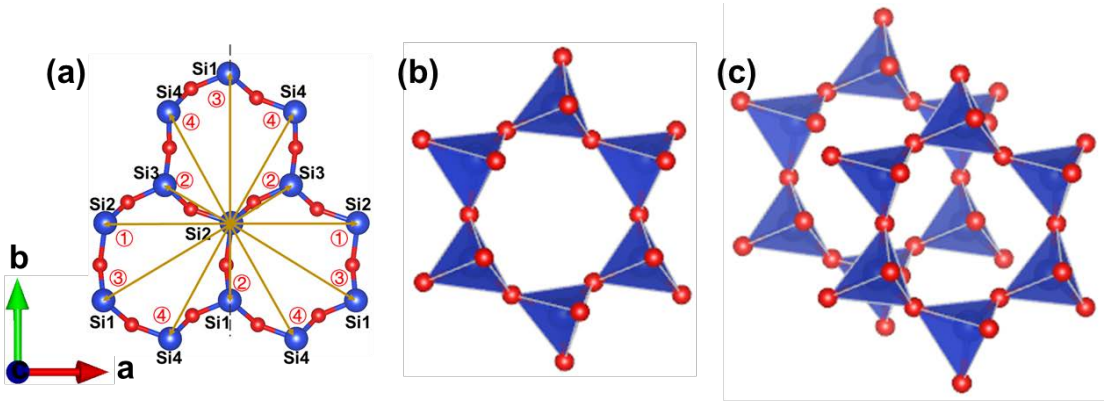

FIGURE 6. Characteristic stacking states of kaolinite, the first layer does not move, and the second layer slides according to the marks in the figure (a), zero shift stacking marked with ①④ (b), $p\vec{b}/3$ stacking marked with ②③ (c).

This is the peer-reviewed, final accepted version for American Mineralogist, published by the Mineralogical Society of America.
The published version is subject to change. Cite as Authors (Year) Title. American Mineralogist, in press.
DOI: https://doi.org/10.2138/am-2022-8830. http://www.minsocam.org/

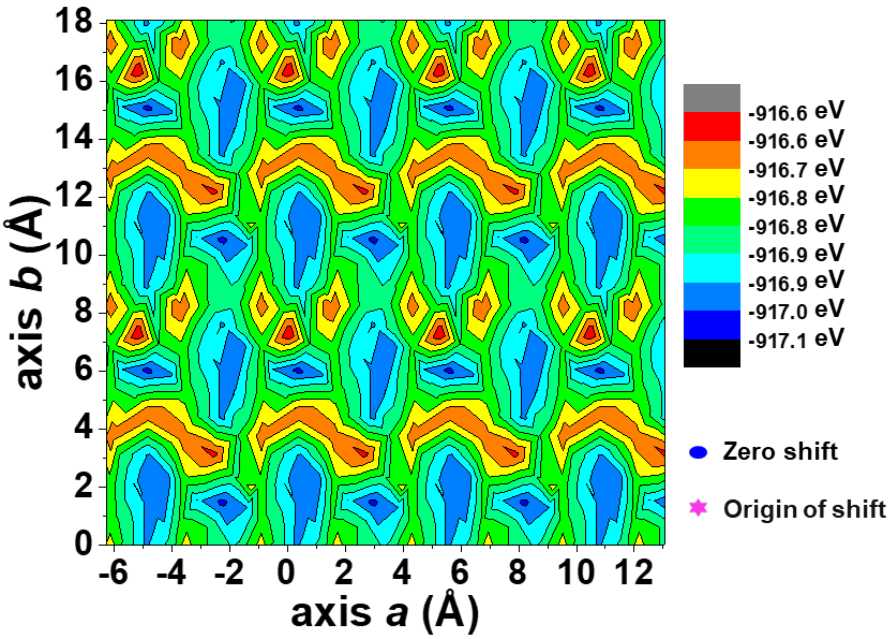

FIGURE 7. Potential energy surface of kaolinite under different stacking states. The more ordered the stacking, the lower the lattice energy. Therefore, ordered stacking can be obtained by characterizing the lattice energy of stacking.

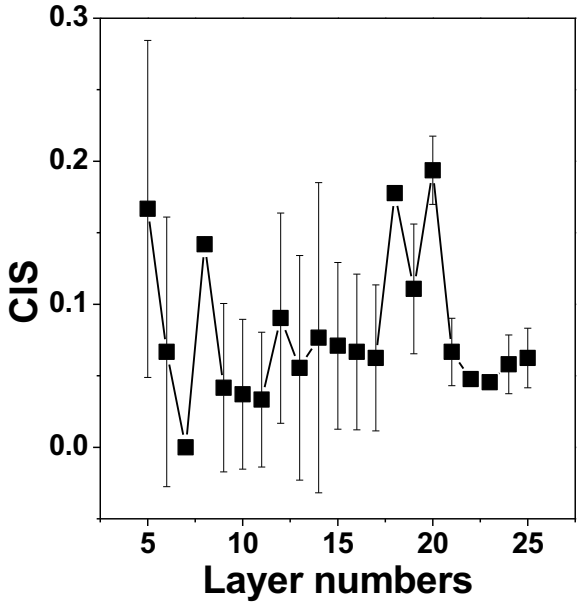

FIGURE 8. Effect of stacking layers on the CIS to find the optimal number of layers for structure refinement.

This is the peer-reviewed, final accepted version for American Mineralogist, published by the Mineralogical Society of America.
The published version is subject to change. Cite as Authors (Year) Title. American Mineralogist, in press.
DOI: https://doi.org/10.2138/am-2022-8830. http://www.minsocam.org/

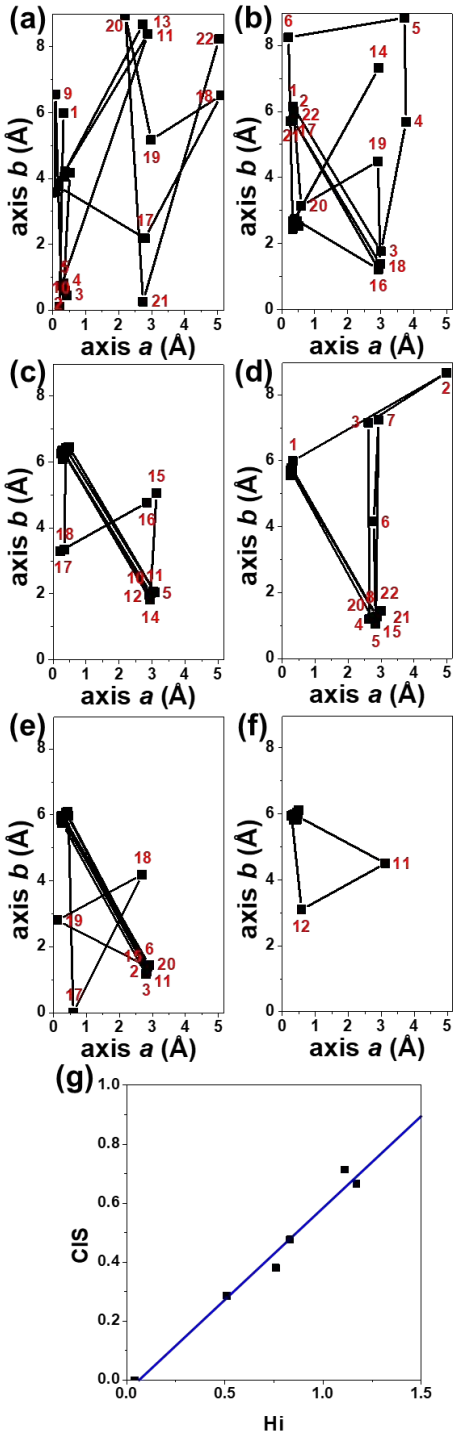

FIGURE 9. Projection of each kaolinite layer on plane *a*–*b* to visualize the displacement of the layers, KL1–KL6 (a–f), and a fitting plot of CIS against Hi to prove that Hi is mainly affected by the stacking order–disorder in kaolinite (g).

This is the peer-reviewed, final accepted version for American Mineralogist, published by the Mineralogical Society of America.
The published version is subject to change. Cite as Authors (Year) Title. American Mineralogist, in press.
DOI: https://doi.org/10.2138/am-2022-8830. http://www.minsocam.org/

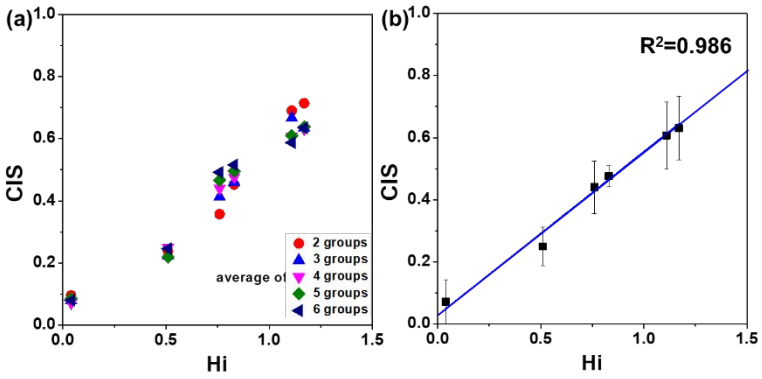

FIGURE 10. Influence of times of structure refinement on the correlation between Hi and CIS (a), and a linear fitting of CIS (the average of four repeated structural refinements) against Hi (b).